Forest Ecology and Management 473 (2020) 118305

Contents lists available at ScienceDirect

Forest Ecology and Management

journal homepage: www.elsevier.com/locate/foreco

Intraspecific variation in functional wood anatomy of tropical trees caused by effects of forest edge

Warlen Silva da Costa[a], Maura Da Cunha[a,*], Pablo José F. Pena Rodrigues[b], Mariana de Andrade Iguatemy[b], Fernando Valladares[c,d], Claudia Franca Barros[b]

[a] Laboratório de Biologia Celular e Tecidual, Centro de Biociências e Biotecnologia, Universidade Estadual do Norte fluminense Darcy Ribeiro, CEP 28035-200, Campos dos Goytacazes, RJ, Brazil

[b] Diretoria de Pesquisas, Instituto de Pesquisas Jardim Botânico do Rio de Janeiro, CEP: 22460-030, Rio de Janeiro, RJ, Brazil

[c] Laboratorio Internacional de Cambio Global (LINC-Global), Museo de Ciencias Naturales MNCN-CSIC, Madrid, Spain

[d] Departamento de Biología y Geología, Escuela Superior de Ciencias Experimentales y Tecnológicas, Universidad Rey Juan Carlos, Móstoles, Spain

ARTICLE INFO

Keywords:
Functional anatomy
Linear canopy openings
Tree
Phenotypic plasticity
Wood anatomical strategies
Wood anatomical traits

ABSTRACT

Forest edge effects promote striking microclimatic shifts that result in greater light exposure, increased air temperature and evapotranspiration rates, and reduced soil moisture can alter stem hydraulic conductivity. These environmental conditions greatly increase the risk of emboli in xylem, which can disrupt or even cease water transport. We investigated tropical tree species in contrasting sites to understand the influence that edge effects have on wood functional anatomy. We compared wood anatomical traits between trees of forest edge and forest interior sites. The species exhibited two types of xylem arrangements based on the distribution of parenchyma cells: *Pseudopiptadenia inaequalis* and *Copaifera lucens*, with paratracheal axial parenchyma (PP), and *Eugenia excelsa* and *Erythroxylum cuspidifolium*, with predominant apotracheal axial parenchyma (AP). Tree species with PP xylem possessed shorter and wider vessel elements and lower ray and vessel frequencies, while species with AP xylem possessed longer and narrower vessel elements and higher ray and vessel frequencies. Regardless of the axial parenchyma arrangement, all four species had a greater percentage of axial parenchyma at the edge sites. The different xylem arrangements showed distinct responses to the edge effect in vessel frequency. The tropical tree species studied here shift to a greater abundance of axial parenchyma when subjected to effects of forest edge, probably to ensure safe water transport. This behavior, in the face of environmental stresses, is a plastic response, and likely due to functional versatility of parenchyma cells. The patterns of vessel frequency for PP and AP suggest that these xylem arrangements can be considered functional groups since the species in each group share similar traits and have similar strategies for conducting and maintaining water flow.

1. Introduction

The Atlantic Forest is characterized by high levels of species diversity and endemism (Galindo-Leal and Câmara, 2005), and represents one of the 36 global biodiversity hotspots (Mittermeier et al., 2004; Scarano and Ceotto, 2015; Weinzettel et al., 2018). Deforestation, resulting from historical human occupation has left only 28% of the original extent of the Atlantic Forest (Rezende et al., 2018). Most remnants are isolated pockets that are restricted to slopes away from anthropic habitats (Silva et al., 2007; Metzger et al., 2009) as is the case for “Serra do Mar”, where only 36.5% of the original forest remains (Ribeiro et al., 2009). Forest fragmentation and edge effects occur in many Atlantic Forest sites and significantly alter natural forest patterns and processes (Rodrigues et al., 2016; Prieto et al., 2013). Forest edge effects seem to speed up forest dynamics and promote high tree mortality and less recruitment (Rodrigues et al., 2016). Briefly, anthropogenic edge effects show complex cause-consequence outcomes and may represent an actual threat to species survival. In this way, it is very important to understand the manner in which species respond to these changes.

Trees that survive at forest edges are subjected to wind turbulence, which results in higher coverage by lianas, and a sharp increase in light exposure and evapotranspiration rates (Laurance et al., 2000). Some tropical forests subjected to edge effects, caused by linear canopy openings, showed increased light irradiance and air temperature, vapor-pressure deficit, and decreased soil humidity (Pohlman et al.,

* Corresponding author.
E-mail addresses: warlen_costa@yahoo.com.br (W. Silva da Costa), maura@uenf.br (M. Da Cunha), pablojfpr@hotmail.com (P. José F. Pena Rodrigues), m_iguatemy@hotmail.com (M. de Andrade Iguatemy), valladares@ccma.csic.es (F. Valladares), cbarrosjbrj@gmail.com (C. Franca Barros).

https://doi.org/10.1016/j.foreco.2020.118305
Received 20 March 2020; Received in revised form 1 June 2020; Accepted 2 June 2020

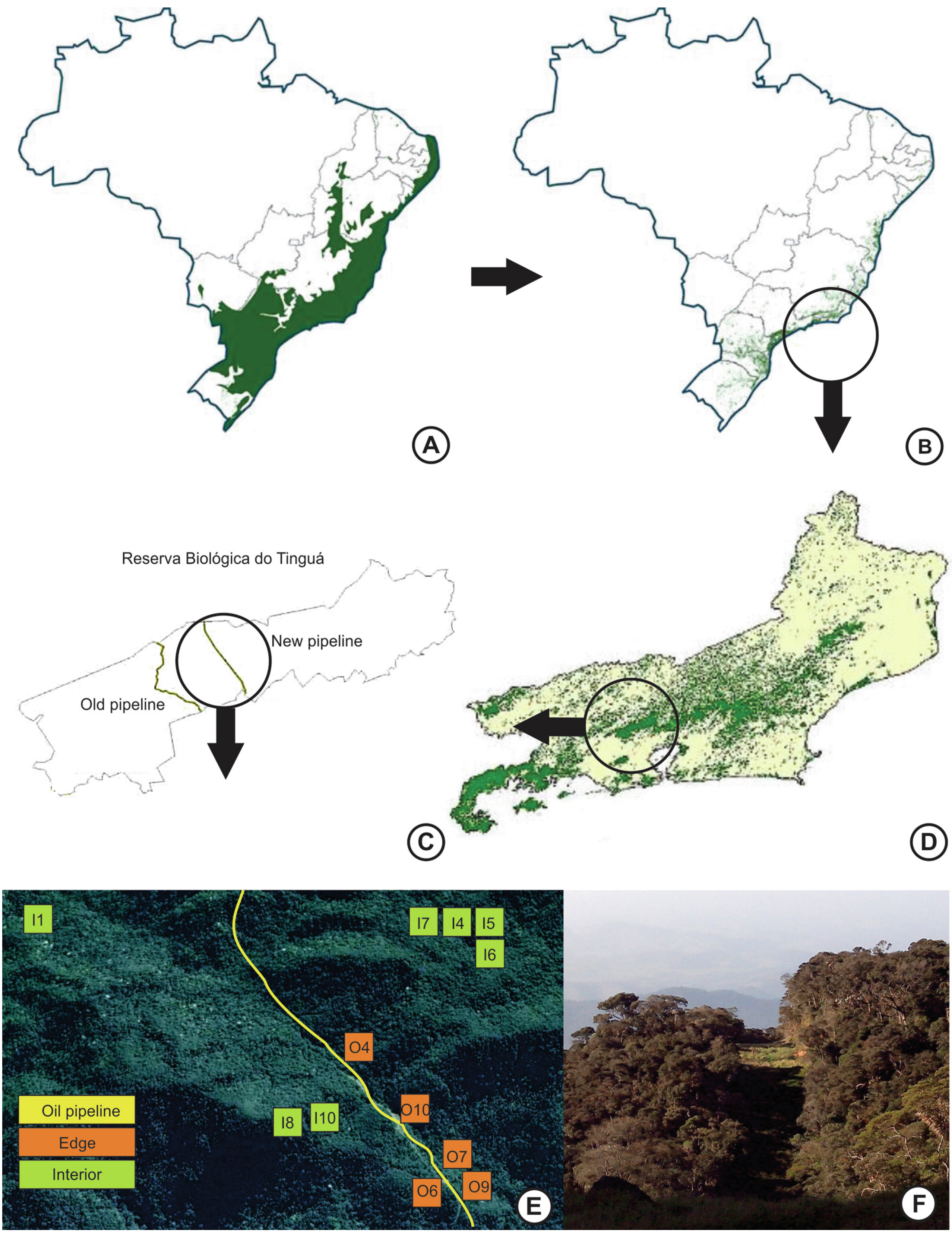

Fig. 1. Study area. A – Atlantic Forest domain. B – Atlantic Forest remnant. C –Map of the Reserva Biológica do Tinguá with the location of the oil pipelines. D – Atlantic Forest fragments in the state of Rio de Janeiro. E – Study area. Plots that are under edge effects are in orange, control areas are in green and the linear canopy opening where the oil pipeline passes is in yellow. F – Linear canopy opening where the oil pipeline passes underground. (For interpretation of the references to colour in this figure legend, the reader is referred to the web version of this article.)

2007). In the Atlantic Forest, such linear edges can also alter the species composition of the understory (Prieto et al., 2013). Habitat fragmentation can sometimes reduce local biodiversity by up to 75% and impair key ecosystem functions by reducing biomass and affecting nutrient cycles (Haddad et al., 2015).

All of these habitat-wide alterations may be linked to the capacity of genotypes to express different phenotypes when exposed to environmental change (i.e., phenotypic plasticity; see Bradshaw, 1965). This important mechanism is quick and ubiquitous for a wide range of organisms that face environmental challenges (Aubin et al., 2016). Trees, when exposed to an unfamiliar environment, must accommodate a large number of changes in the morphology and function of cells, resulting in change in the configuration of tissues and organs (Lachenbruch and McCulloh, 2014). Although phenotypic changes of leaves induced by changes in biotic and abiotic factors have been widely documented, far less is known about the capacity of woody anatomy to accommodate such changes, despite its central role in adjusting the water economy of the entire tree to new conditions (Gratani, 2014).

Sensitivity of the vascular cambium to environmental conditions, and the consequent changes in xylem structure, represents an example of phenotypic plasticity (*sensu* Gianoli and Valladares, 2012), and has been documented in the literature (e.g. Carlquist, 1977, 1988; Baas and Schweingruber, 1987; Wheeler and Baas, 1991; Alves and Angyalosy-Alfonso, 2000; Fonti et al., 2010; Beckman, 2016). Vessel diameter is the wood anatomical trait most subject to structural change and is used most widely as a proxy for hydraulic conductivity (e.g. Poorter et al., 2010; Zanne et al., 2010; Apgaua et al., 2017), according to the Hagen-Poisselle law, which describes that conduit hydraulic conductivity is proportional to its diameter raised to the fourth power. However, the lessor-explored parenchyma cells are speculated to have an important role in the restoration of hydraulic conductivity and in the blockage of air propagation throughout vessels via tyloses (Sun et al., 2008; Brodersen and McElrone, 2013; Carlquist, 2015, 2018; Morris et al., 2016a, 2019; Plavcová et al., 2016; Jupa et al., 2016; Brodersen et al., 2019). Currently, hydraulic conduction is not only understood as a physical process, but also as a complex process involving the participation of living cells associated with vessels, such as parenchyma cells (Morris et al., 2018).

There are two types of parenchyma in hardwood tissue: axial parenchyma, which is oriented vertically in the xylem, and radial parenchyma, which is oriented horizontally in the xylem (Carlquist, 2018). Axial parenchyma can be subdivided into paratracheal parenchyma, which are parenchyma cells positioned around a vessel, and apotracheal parenchyma, which are parenchyma cells distributed diffusely throughout the wood (Morris and Jansen, 2016). This classification has been used in the identification of different taxonomic groups (Metcalfe and Chalk, 1950) and is functionally important since these arrangements are thought to have different associations (Morris and Jansen, 2016). As a general rule, research has shown that species with large vessels have more paratracheal axial parenchyma, whereas species with narrow vessels have more apotracheal parenchyma (Morris et al., 2018). These kinds of axial parenchyma arrangements together with vessel diameter describe distinct xylem patterns that are anatomically and functionally integrated (Morris et al., 2018).

According to Violle et al. (2007), functional groups are groups of species that not only share morphological, physiological, and phenological characteristics but also those that respond similarly to a given environmental condition. We aimed to address how tropical trees respond to the effects of forest edge in terms of their functional wood anatomy. We intended to (1) delimit xylem arrangements and test two hypotheses (2) that species with different xylem arrangements represent distinct functional groups that will respond differently to edge effects, and (3) that parenchyma cells, because of their phenotypic plasticity, will be a determining factor for these differences.

2. Materials and methods

2.1. Study sites

The present study was conducted in Reserva Biológica do Tinguá (22°22′20″ – 22°45′00″ S; 43°40′00″ – 43°05′40″ W), in the state of Rio de Janeiro, Brazil (Fig. 1A-D). The reserve is crossed by the ORBEL 2 oil pipeline, which creates linear canopy openings and promotes edge effects on local vegetation. Twelve permanent sites (300 m2 per site) were installed in Reserva Biológica do Tinguá in 2003 and 2007 (Fig. 1E-F) and have been monitored over the past 10 years (Rodrigues et al., 2008; Simões de Jesus, 2009; Rodrigues et al., 2016). Five sites are located 5 m from the oil pipeline, in an area under edge effects (edge sites), while the other seven are located more than 400 m away, in a control area (interior sites) (Rodrigues et al., 2008).

2.2. Selected species

Four species were selected in 2015 according to the importance value (IV) for the interior sites (Simões de Jesus, 2009); occurrence in both areas (interior and edge); the presence of three individuals for each species, both for interior and edge; and knowledge of the distribution of axial parenchyma for the taxonomic groups involved (Metcalfe and Chalk, 1950). Two xylem arrangements were delimited based on the distribution/location patterns of axial parenchyma relative to vessels, *Pseudopiptadenia inaequalis* (Benth.) Rauschert (Fabaceae Lindl.) and *Copaifera lucens* Dwyer (Fabaceae Lindl.) possess predominantly axial paratracheal parenchyma (PP) (Fig. 2A), while *Eugenia excelsa* O. Berg (Myrtaceae Juss.) and *Erythroxylum cuspidifolium* Mart. (Erythroxylaceae Kunth.) possess predominantly apotracheal parenchyma (AP) (Fig. 2B). Selected individuals had a diameter at breast height (DBH) of at least 8 cm, and a straight stem and trunk without apparent deformation. The DBH was measured, and the height estimated (Table 1) for each individual tree. Since trees from interior sites are taller than trees from edge sites, the effects of tree height on wood anatomy (Olson and Rosell, 2013; Olson et al., 2014) were reduced by standardizing the height range of individuals collected between sites edge and interior sites (Table 1) with the average height of 8.4 m (± 2.9) for *E. cuspidifolium*, 12 m (± 4.8) for *E. excelsa*, 12.5 m (± 4.6) for *P. inaequalis* and 14.8 m (± 6.5) for *C. lucens*. Twenty-nine individuals met our selection criteria (Table 1), fourteen from interior sites and fifteen from edge sites. Wood samples were collected from these trees at breast height (ca. 1.30 m from the soil) using a Pressler increment borer (Grissino–Mayer, 2003), which is a non-destructive method of wood collection (Barros et al., 2001). The surplus of each of the twenty-nine wood samples not used in this study approximately five centimeters, was deposited in the wood collection of Universidade Estadual do Norte Fluminense Darcy Ribeiro – Xiloteca Dra. Cecília Gonçalves Costa (HUENFw), with replicates deposited in the wood collection of Instituto de Pesquisas Jardim Botânico do Rio de Janeiro (RBw) (Table 1).

2.3. Wood anatomy

The twenty-nine wood samples were immersed in Franklin solution (Jane, 1956) to dissociate cell elements, and then stained with 1% aqueous safranin and mounted with 50% glycerin on semi-permanent slides (Strasburger, 1924) for the measurement of individual cells (fibres and vessel elements). Histological sections were prepared by boiling samples in a water-glycerin mix (1:1) for softening. Transversal, tangencial and radial sections, with thicknesses ranging from 16 to 30 μm, were then made using a Leica sliding microtome (Burger and Richter, 1991). The three histological sections obtained for the wood of each individual tree were then clarified and stained with safranin and astra blue (Bukatsch, 1972), dehydrated and mounted with synthetic resin (Johansen, 1940; Sass, 1958). Images, taken with an Olympus

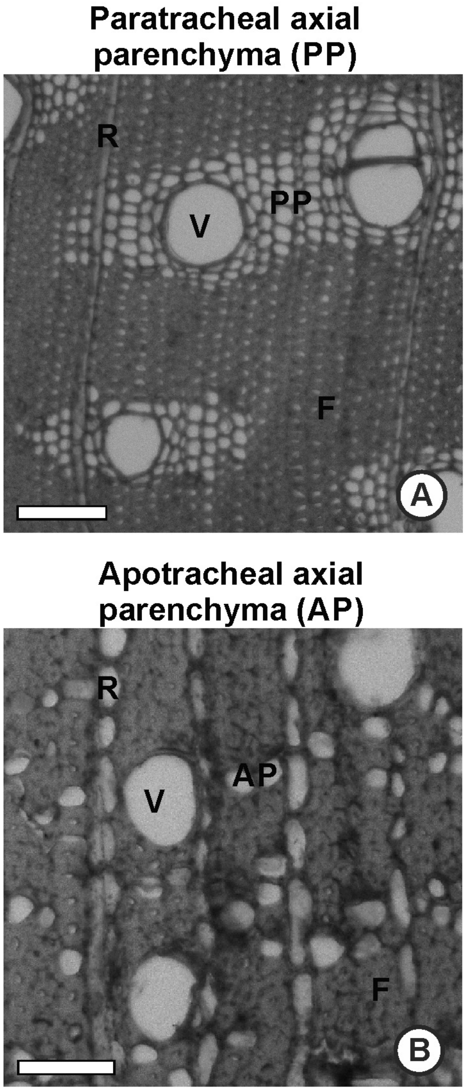

Fig. 2. Functional groups based on axial parenchyma distribution. A – Group with paratracheal parenchyma represented by transversal section of *P. inaequalis* (Bar = 100 μm). B – Group with apotracheal parenchyma represented by transversal section of *E. excelsa* (Bar = 50 μm). V = vessel, F = fibre, R = ray, PP = paratracheal parenchyma, AP = apotracheal parenchyma.

DP73 camera attached to an Olympus BX50 microscope, were analyzed using the software Image Pro Plus v. 4.0 for Windows. All measurements and descriptions for vessels, fibres, parenchyma and rays followed the recommendations of the IAWA Committee (1989). Vessel area was estimated with three points distributed throughout the vessels, for a total of 25 measurements for each individual tree. Tissue percentages were measured with a grid of 100 random points for each one of the 10 images of the transversal section of wood of each individual tree. Measurements for both vessel area and tissue percentages were performed using the software Image Pro Plus v. 4.0 for Windows.

2.4. Statistical analyses

Comparisons of tree wood anatomy between edge and interior sites were performed using analysis of variance (ANOVA) followed by Tukey tests (for all tests $\alpha = 0.05$), for each quantitative variable. The phenotypic plasticity index (PPI) and the phenotypic variability index (PVI) were calculated for the anatomical variables of each species in order to evaluate the degree of plasticity and variability, respectively, of each quantitative variable for the studied sites (Valladares et al., 2006; Gianoli and Valladares, 2012), using the following expressions:

$PPI = \frac{M-m}{M}$ $PVI = \frac{Max-Min}{Max}$ where *PPI* is phenotypic plasticity index and *PVI* is phenotypic variability index; *M* is maximum mean value; *m* is minimum mean value; *Max* is the maximum value; *Min* is the minimum value. PVI was calculated for edge and interior sites separately, and then a total PVI was calculated for both together for the same variables.

Based on the anatomical values obtained, vulnerability (VI) and mesomorphy (MI) indeces were calculated according to Carquist (1977), using the following expressions:

$$VI = \frac{\bar{x}VD}{\bar{x}VF} \quad MI = \frac{VI}{\bar{x}LVE}$$

where *VI* denotes vulnerability index and *MI* denotes the mesomorphic index; *VD* is diameter of vessels (μm); *VF* is frequency of vessels (mm^2); *LVE* is length of vessel elements (μm). Mesomorphy index was calculated to determine the degree of mesomorphism or xeromorphism of the species, with values above 200 indicating mesophytes (Carlquist, 1977). The vulnerability index indicates the degree of vulnerability of the conducting tissue to embolism formation, therefore, values below 1.0 show greater safety under conditions of water stress (Carlquist, 1977).

Finally, a factorial ANOVA with three hierarchical levels (edge/interior, species and individuals) was performed to investigate the relationship between the selected species and the study sites and to understand general tendencies in the wood anatomy of these species. Prior to the ANOVA, normality and homogeneity of variance were tested by the Shapiro-Wilk test and the Levene test, respectively (Zar, 2010). All statistical tests were performed with the statistical package R (R Core Team, 2018) and the software Statistica 7 (StatSoft, 1993).

3. Results

Anatomical analysis of the wood of the studied species provided other characteristics that make the delimitation of xylem arrangements more robust. Thus, the xylem arrangement of the PP species was found to have shorter and wider vessel elements and lower ray and vessel frequencies (Fig. 3/ Fig. 4 A-D). The xylem arrangement of the AP species is characterized by longer and narrower vessel elements and higher ray and vessel frequencies (Fig. 3/ Fig. 4 A-D). A higher vulnerability index was found for PP species, *P. inaequalis* (8.8 and 4.9) and *C. lucens* (19.4 and 16.6) from interior sites and edge sites, respectively, when compared with AP species, *E. excelsa* (1.3 and 1.6) and *E. cuspidifolium* (0,6 and 0.9) from interior sites and edge sites respectively (Table 2). The mesomorphy index was greater than 200 for all species (Table 2). Complete anatomical descriptions are provided in the Supplementary data.

Qualitative characters were important in the anatomical identity of each species and in the delimitation of xylem arrangements (parenchyma type PP or AP), but they did not exhibit differences between individuals from the edge and the interior (Fig. 3). However, some quantitative characters exhibited differences between individuals from these different sites. When individuals of edge sites were compared to those of interior sites, all species possessed a higher percentage of axial parenchyma cells ($P < 0.05$) for individuals from edge sites (26.95% to 37.73%) than for individuals from interior sites (17.60% to 23.13%), and a lower percentage of fibres at edge sites for most of the species (Fig. 4 E-F; Fig. 5 A-B; Table 2).

The individuals of each xylem arrangement type differed between edge and interior ($P < 0.05$). For PP species, individuals from the edge had higher vessel frequencies (17 vessels/mm^2 and 7 vessels/mm^2, for *P. inaequalis* and *C. lucens*, respectively) than individuals from the interior (14 vessels/mm^2 and 5 vessels/mm^2, respectively; Fig. 5C; Table 2). For AP species, individuals from the edge had lower vessel frequencies (36 vessels/mm^2 and 66 vessels/mm^2, for *E. excelsa* and *E cuspidifolium*, respectively) than individuals from the interior (45 vessels/mm^2 and 98 vessels/mm^2, respectively; Fig. 5C; Table 2).

Table 1
Data on collected species, families, importance value (IV), number of individuals, collection site, diameter at breast height (DBH), estimated height (m), ecological classification, life form and wood collection information (RBw and HENFw).

Family	Species	IV	Individuals	Sites	Plots	DBH (cm)	Heigth (m)	Ecological classification	Canopy structure	RBw	HENFw
Fabaceae	*P. inaequalis*	3,104	15	Interior	I1	20.7	16.2	Late secondary	Canopy tree	10,409	289
			489	Interior	I8	11.6	16.2	Late secondary	Canopy tree	10,410	213
			636	Interior	I10	34	18	Late secondary	Canopy tree	10,411	277
			386	Edge	O6	13.5	9	Late secondary	Canopy tree	10,412	201
			410	Edge	O6	10	7.2	Late secondary	Canopy tree	10,413	191
			450	Edge	O7	8.8	7	Late secondary	Canopy tree	10,414	212
			668	Edge	O10	18.6	14.4	Late secondary	Canopy tree	10,415	276
	C. lucens	2,157	261	Interior	I5	11.7	19.8	Late secondary	Canopy tree	10,416	311
			286	Interior	I5	9	9	Late secondary	Canopy tree	10,417	312
			302	Interior	I5	21.1	18	Late secondary	Canopy tree	10,418	313
			289	Edge	O4	17.9	21.6	Late secondary	Canopy tree	10,419	361
			599	Edge	O9	25.8	19.8	Late secondary	Canopy tree	10,420	124
			677	Edge	O10	54.53	10.5	Late secondary	Canopy tree	10,421	125
			686	Edge	O10	21.3	5	Late secondary	Canopy tree	10,422	126
Myrtaceae	*E. excelsa*	4,395	346	Interior	I6	22.6	21.6	Late secondary	Canopy tree	10,423	326
			496	Interior	I8	18.2	12.6	Late secondary	Canopy tree	10,424	344
			644	Interior	I10	19.4	12.6	Late secondary	Canopy tree	10,425	169
			684	Interior	I10	10.6	9	Late secondary	Canopy tree	10,426	351
			489	Edge	O7	8.3	9	Late secondary	Canopy tree	10,427	167
			496	Edge	O7	23	15	Late secondary	Canopy tree	10,428	368
			593	Edge	O9	13.7	10.8	Late secondary	Canopy tree	10,429	168
			671	Edge	O10	8.5	5.4	Late secondary	Canopy tree	10,430	170
Erythroxylaceae	*E. cuspidifolium*	3,224	176	Interior	I4	9.1	7.2	Initial secondary	Understorye tree	10,431	304
			361	Interior	I6	11.1	14.4	Initial secondary	Understorye tree	10,432	325
			402	Interior	I7	8.6	7.2	Initial secondary	Understorye tree	10,433	335
			468	Interior	I8	8.7	9	Initial secondary	Understorye tree	10,434	343
			408	Edge	O6	13	9	Initial secondary	Understorye tree	10,435	129
			433	Edge	O7	8.08	5.4	Initial secondary	Understorye tree	10,436	164
			459	Edge	O7	8.2	7	Initial secondary	Understorye tree	10,437	165

The most plastic traits were percentage of axial parenchyma (0.17 to 0.39), percentage of fibres (0.21 to 0.32) and vessel frequency (0.19 to 0.32) (Fig. 6; Table 2). Furthermore, the percentage of fibres and axial parenchyma had higher total PVI than the those calculated separately for each site (Fig. 6; Table 2). Differences between total PVI and PVI calculated separately for the edge and interior reflect the variability that these anatomical characteristics possess when submitted to different environmental conditions. The variables of approximate vessel area, vessel height, ray width, fibre lumen width and parenchyma series height in number of cells had highest PVI values among individuals from the same site (interior or edge), which influenced the total index, indicating that variation in these variables is not related to edge effects (Table 2).

The linear regression and Spearman correlation between PVI and PPI of the analyzed species were not significant (*P* greater than 0.05), as the anatomical traits varied differently (Table 2; Fig. 7). In summary, the main results show that the xylem arrangements exhibited higher parenchyma percentage in edge individuals and distinct trends for vessel frequency, with it higher for PP individuals from the edge than from the interior, while the inverse was true for AP species.

4. Discussion

The xylem arrangements proposed here (AP and PP) are consistent with general arrangements based on axial parenchyma type and its relation with vessels in woody angiosperms (Morris et al., 2018). Therefore, our results confirm a close relationship between parenchyma distribution and vessel diameter, constituting distinct xylem arrangements that are found in several species of different taxonomic groups (Morris et al., 2018). Although both xylem arrangements responded to edge effects with an increase in the amount of axial parenchyma, they differed in their response pattern for vessel frequency. This difference suggests that these xylem arrangements can be considered functional groups *sensu* Violle et al. (2007), since they are groups comprising species that share similar traits and have similar strategies for conduction and maintenance of water flow. Xylem is not simply a tissue for water conduction by physical processes, but comprises distinct cell types that function in an integrated matter for water conduction (Morris et al., 2016b, 2018; Carlquist, 2015, 2018).

A general trend was observed in all the studied species: an increase in the percentage of axial parenchyma and a decrease in the percentage of fibres in individuals from edge sites. In tropical trees, parenchyma cells are associated with water storage, especially for species that occur in areas with high evaporation rates, as observed for *Ceiba pentandra* (L.) Gaertn (Plavcová et al., 2016) from tropical forests and *Stryphnodendron polyphyllum* Mart. and *Vochysia tucanorum* Mart. from Cerrado (Sonsin et al., 2012). The capacity to store water in parenchyma cells, and its release in the transpiration stream, is an important mechanism for maintaining hydraulic flow in xylem (Jupa et al., 2016). The results show that an increase in the proportion of parenchyma is an efficient survival mechanism for trees under edge effects. The greater percentage of fibres in individuals from interior sites was expected due to the negative correlation between fibres and parenchymatic cells documented in all biomes, but especially in tropical regions (Morris et al., 2016b).

According to Bastias et al. (2017), plants of highly diverse communities can have functional similarities. This is possible because intraspecific variation in characteristics does not decrease with increasing biodiversity, as proposed by classic niche theory (MacArthur and Levins, 1967). In general, the phenotypic plasticity and variability indexes of the wood traits analyzed here varied little in among species, which can be understood because of neutral ecosystem processes (Bastias et al., 2017). However, we found greater percentages of parenchyma in edge individuals and differences in vessel frequency between xylem arrangements.

All of the studied species are mesomorphic according to Mesomorphy index (Carlquist, 1977). However, the Vulnerability index shows that the relationship between vessel frequencies and vessel diameters exhibited distinct tendencies according to the xylem arrangements of the studied species. PP species possess wider and shorter vessels that conduct larger volumes of water (Sperry et al., 2006), but

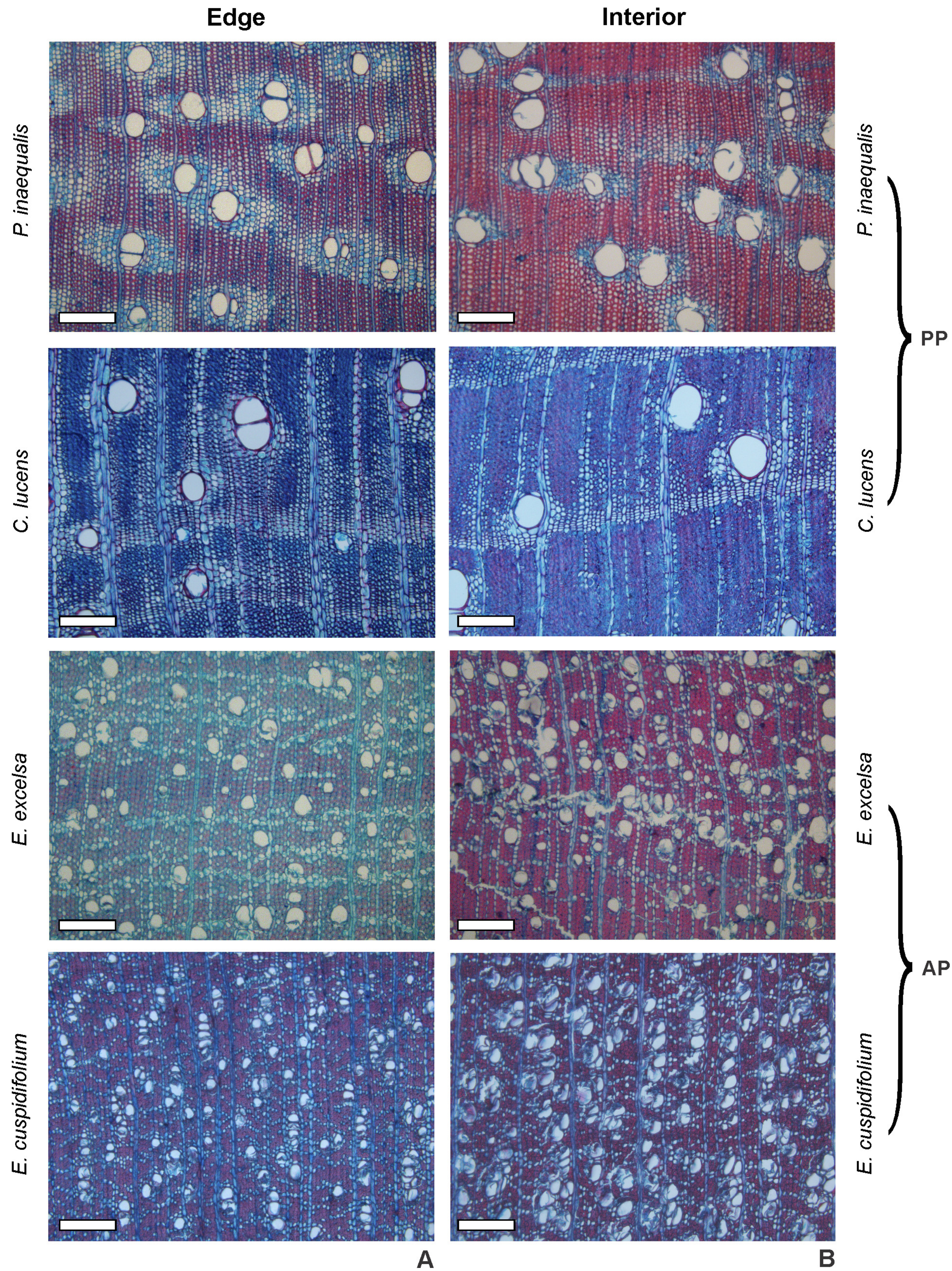

Fig. 3. Transversal images of wood from individuals in the edge (A) and in the interior (B). Bar = 200 µm.

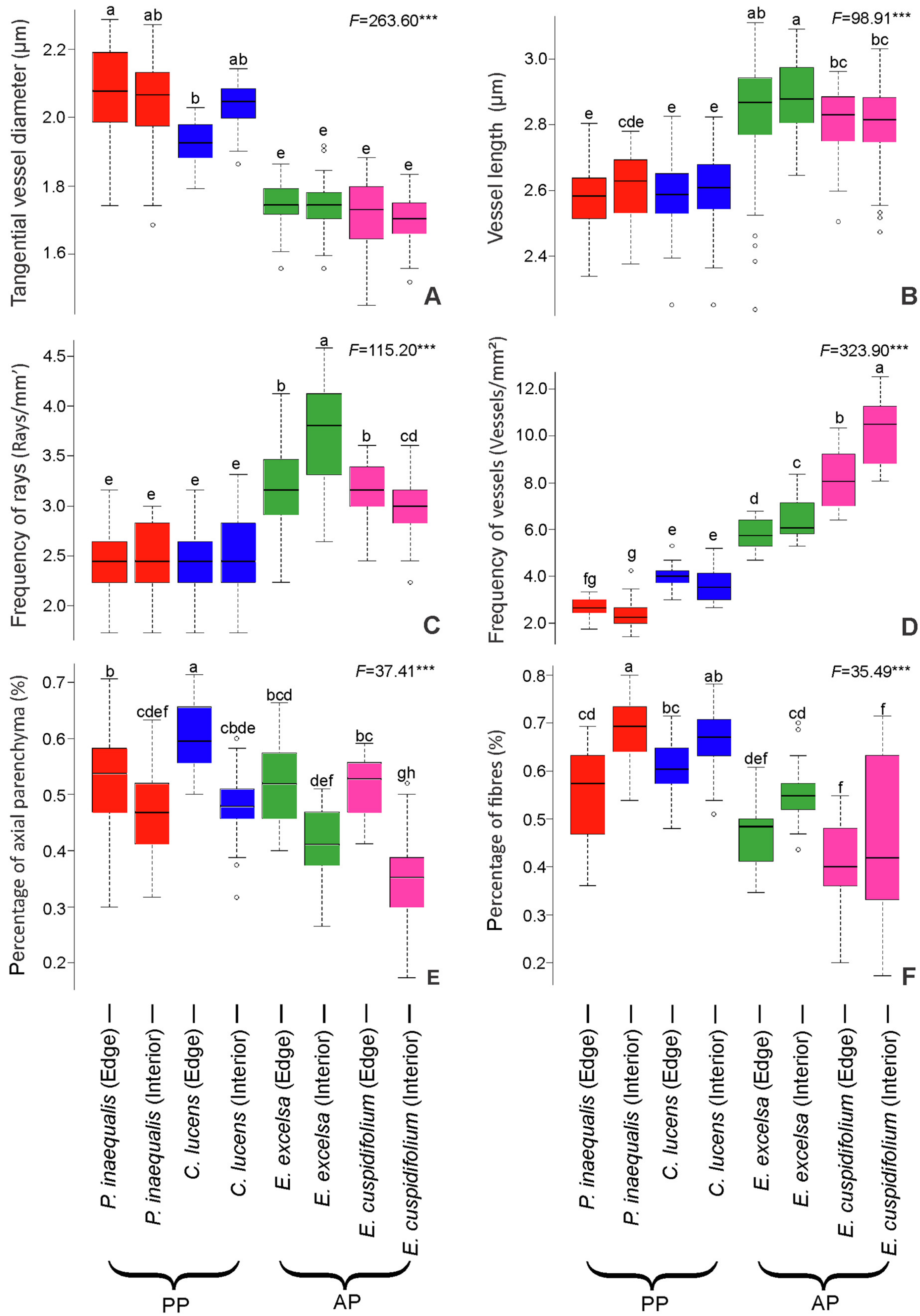

Fig. 4. Boxplots presenting: tangential vessel diameter (A), vessel length (B), ray frequency/mm' (C), vessel frequency/mm2, (D) axial parenchyma percentage (E) and fibre percentage (F). Each box encompasses the 25th to 75th percentiles; the median is indicated by the boldest vertical line while the other vertical lines outside the box indicate the maximum and minimum. Dots indicate outliers. One-way ANOVAs were performed and significant differences between groups are indicated by different letters based on Tukey Honestly Significant Difference test at a 0.05 confidence level.

Table 2
List of quantitative variables investigated in each species. For each variable, the minimum values (MIN), average (M), maximum (MAX), standard deviation (SD), phenotypic plasticity index (PPI) and phenotypic variability index (PVI) in each site (edge and interior) are presented. The vulnerability, mesomorphy and total PVI indices are also presented.

Species	*P. inaequalis*											
Sites	Edge					Interior					Total PVI	PPI
Quantitative variables	PVI	MIN	M	MAX	SD	PVI	MIN	M	MAX	SD		
Vessel frequency (Vessels/mm^2)	0.7	9.0	17.8	32.0	4.9	0.8	7.0	14.5	32.0	6.7	0.8	0.2
Length vessel (µm)	0.7	176.7	393.7	666.4	88.9	0.7	176.7	384.9	649.0	97.0	0.7	0.0
Vessel tangential diameter (µm)	0.5	60.0	84.7	116.5	12.4	0.6	60.0	99.9	137.6	18.6	0.6	0.2
Vessel radial diameter (µm)	0.5	65.6	95.6	131.2	14.6	0.6	65.6	118.2	156.8	21.6	0.6	0.2
Estimated vessel area (µm)	0.7	3379.0	6717.0	11917.9	1889.1	0.8	3379.0	9919.8	18141.2	3457.0	0.8	0.3
Vessel wall thickness (µm)	0.6	2.0	3.0	4.7	0.5	0.6	1.9	3.2	4.8	0.6	0.6	0.1
Intervessel pit heigth (µm)	0.3	4.1	4.7	5.7	0.4	0.4	2.9	4.2	5.0	0.6	0.5	0.1
Intervessel pit width (µm)	0.2	4.9	5.3	6.2	0.5	0.4	3.3	4.4	5.9	0.8	0.5	0.2
Vessel-ray pit heigth (µm)	**0.3**	3.8	4.6	5.8	0.5	**0.4**	2.6	3.5	4.1	0.4	**0.6**	0.2
Vessel-ray pit width (µm)	0.3	3.6	4.3	5.2	0.4	0.2	3.6	4.0	4.6	0.3	0.3	0.1
Vessel-parenchyma pit heigth (µm)	0.2	3.7	4.2	4.7	0.3	0.3	2.9	3.7	4.2	0.4	0.4	0.1
Vessel-parenchyma pit width (µm)	0.4	4.1	5.2	6.8	0.8	0.3	3.6	4.1	4.9	0.3	0.5	0.2
Fibre diameter (µm)	0.5	14.1	19.7	30.1	3.3	0.5	14.6	19.9	27.5	2.9	0.5	0.0
Fibre lumina (µm)	0.8	5.3	12.0	25.0	3.7	0.5	8.3	11.5	18.0	2.3	0.8	0.0
Fibre length (µm)	0.6	635.9	990.3	1520.3	194.1	0.6	680.6	1026.5	1520.3	167.3	0.6	0.0
Fibre wall thickness (µm)	0.6	2.2	3.9	6.0	0.9	0.6	2.5	4.2	5.7	0.7	0.6	0.1
Parenchyma strand length (number of cells)	0.8	1.0	2.1	4.0	0.8	0.8	1.0	1.9	4.0	0.7	0.8	0.1
Parenchyma strand length (µm)	0.7	220.5	454.9	647.5	90.2	0.6	253.9	487.2	696.8	99.4	0.7	0.1
Rays frequency (Rays/mm')	0.7	3.0	6.1	10.0	1.6	0.8	3.0	6.6	12.0	2.0	0.8	0.1
Ray heigth (µm)	0.7	83.2	168.9	270.4	39.5	0.6	113.7	192.4	318.2	48.4	0.7	0.1
Ray width (µm)	0.7	6.6	13.2	20.9	2.5	0.7	6.6	13.1	22.5	3.3	0.7	0.0
Vessels percentage (%)	0.2	11.2	12.6	13.7	1.3	0.5	11.3	16.4	23.1	6.1	0.5	0.2
Fibres percentage (%)	**0.3**	28.7	35.1	42.2	6.1	**0.3**	35.6	44.5	53.5	9.0	**0.5**	0.2
Rays percentage (%)	**0.3**	11.3	14.6	17.1	2.5	**0.3**	13.7	16.0	20.3	3.8	**0.4**	0.1
Axial parenchyma percentage (%)	**0.2**	32.8	37.7	42.3	4.5	**0.2**	21.0	23.1	26.9	3.3	**0.5**	0.4
Wood density (g/cm3)	0.1	0.6	0.6	0.7	0.0	0.2	0.6	0.6	0.7	0.1	0.2	0.0
Vulnerability index	4.9						8.8					
Mesomorphy index	1937.4						3506.1					

Species	*C. lucens*											
Sites	Edge					Interior					Total PVI	PPI
Quantitative variables	PVI	MIN	M	MAX	SD	PVI	MIN	M	MAX	SD		
Vessel frequency (Vessels/mm^2)	0.8	3.0	7.9	19.0	3.1	0.9	2.0	5.9	18.0	3.4	0.9	0.3
Length vessel (µm)	0.8	111.6	360.9	634.5	99.1	0.6	236.1	418.6	601.7	89.7	0.8	0.1
Vessel tangential diameter (µm)	0.7	54.4	126.7	192.4	32.2	0.7	47.6	112.3	186.0	29.3	0.8	0.1
Vessel radial diameter (µm)	0.7	67.3	154.2	256.1	42.4	0.7	60.8	131.3	242.1	34.4	0.8	0.1
Estimated vessel area (µm)	0.9	4070.5	16778.7	39962.9	8799.4	0.9	2902.6	12609.0	28727.7	6140.4	0.9	0.2
Vessel wall thickness (µm)	0.7	2.7	5.4	9.3	1.2	0.6	2.5	4.6	7.0	1.0	0.7	0.2
Intervessel pit heigth (µm)	**0.3**	5.3	6.7	7.9	0.6	**0.3**	4.5	5.4	6.8	0.8	**0.4**	0.2
Intervessel pit width (µm)	0.3	6.0	7.3	8.1	0.5	0.5	4.5	6.5	9.3	1.7	0.5	0.1
Vessel-ray pit heigth (µm)	0.4	4.4	5.5	6.8	0.6	0.4	3.9	5.3	6.8	0.9	0.4	0.0
Vessel-ray pit width (µm)	0.3	5.0	6.0	7.1	0.6	0.5	4.0	5.9	7.9	1.4	0.5	0.0
Vessel-parenchyma pit heigth (µm)	0.3	4.1	5.1	6.0	0.4	0.3	4.1	5.0	5.8	0.5	0.3	0.0
Vessel-parenchyma pit width (µm)	0.3	5.9	7.0	8.6	0.7	0.6	4.1	6.6	9.3	1.4	0.6	0.1
Fibre diameter (µm)	0.7	7.7	19.3	26.9	3.5	0.6	10.3	18.9	24.5	2.9	0.7	0.0
Fibre lumina (µm)	0.8	3.3	10.8	20.0	4.1	0.9	2.1	8.8	17.3	3.7	0.9	0.2
Fibre length (µm)	0.7	575.3	1130.6	1914.2	257.7	0.6	707.3	1183.0	1780.4	202.9	0.7	0.0
Fibre wall thickness (µm)	0.7	2.0	4.3	7.5	1.3	0.6	3.0	5.0	7.8	1.2	0.7	0.2
Parenchyma strand length (number of cells)	0.8	1.0	3.0	6.0	1.0	0.8	1.0	2.7	4.0	0.8	0.8	0.1
Parenchyma strand length (µm)	0.7	172.5	415.3	630.4	94.9	0.6	211.7	420.5	578.3	86.6	0.7	0.0
Rays frequency (Rays/mm')	0.7	3.0	5.9	10.0	1.3	0.7	3.0	6.4	9.0	1.6	0.7	0.1
Ray heigth (µm)	0.7	232.3	387.7	905.5	108.7	1.0	16.4	392.2	877.2	140.2	1.0	0.0
Ray width (µm)	0.8	16.0	49.0	71.5	11.5	1.0	2.8	34.6	67.5	14.8	1.0	0.3
Vessels percentage (%)	**0.5**	8.5	12.3	16.2	3.7	**0.5**	4.3	7.1	9.1	2.5	**0.7**	0.4
Fibres percentage (%)	0.5	19.9	32.6	40.8	8.9	0.2	41.9	47.0	53.2	5.7	0.6	0.3
Rays percentage (%)	**0.1**	25.9	28.1	30.2	1.8	**0.2**	21.3	23.4	26.2	2.5	**0.3**	0.2
Axial parenchyma percentage (%)	0.4	21.2	27.0	37.2	7.3	0.1	21.2	22.5	24.1	1.5	0.4	0.2
Wood density (g/cm3)	0.2	0.7	0.8	0.9	0.1	0.1	0.8	0.8	0.9	0.0	0.2	0.0
Vulnerability index	16.6					19.4						
Mesomorphy index	6141.3					8299.1						

Species	*E. excelsa*

(*continued on next page*)

Table 2 (*continued*)

Sites	Edge					Interior					Total PVI	PPI
Quantitative variables	PVI	MIN	M	MAX	SD	PVI	MIN	M	MAX	SD		
Vessel frequency (Vessels/mm^2)	**0.6**	22.0	36.1	56.0	8.1	**0.6**	28.0	45.5	70.0	12.5	**0.7**	0.2
Length vessel (µm)	0.9	171.5	727.3	1288.6	216.8	0.7	439.3	820.7	1304.1	200.8	0.9	0.1
Vessel tangential diameter (µm)	0.5	35.2	56.0	72.1	7.9	0.6	35.2	56.1	81.6	9.4	0.6	0.0
Vessel radial diameter (µm)	0.6	40.0	69.0	96.0	10.8	0.5	48.0	69.8	99.4	12.3	0.6	0.0
Estimated vessel area (µm)	0.9	886.5	3245.6	6080.6	872.8	0.7	1575.9	3383.4	6080.6	984.2	0.9	0.0
Vessel wall thickness (µm)	0.5	2.0	2.9	4.2	0.5	0.6	1.7	2.8	4.0	0.4	0.6	0.0
Intervessel pit heigth (µm)	0.3	3.4	4.1	4.8	0.4	0.5	2.9	3.8	5.3	0.8	0.5	0.1
Intervessel pit width (µm)	0.5	2.8	4.1	5.5	0.8	0.4	2.8	3.8	4.3	0.4	0.5	0.1
Vessel-ray pit heigth (µm)	0.4	2.1	2.8	3.3	0.4	0.4	2.4	3.2	4.2	0.6	0.5	0.1
Vessel-ray pit width (µm)	**0.3**	2.4	2.9	3.7	**0.3**	0.4	2.8	3.3	4.4	0.4	**0.4**	0.1
Vessel-parenchyma pit heigth (µm)	0.4	2.3	2.9	3.6	0.3	0.3	2.4	3.0	3.7	0.3	0.4	0.0
Vessel-parenchyma pit width (µm)	0.4	2.0	2.9	3.4	0.4	0.3	2.6	3.1	3.7	0.3	0.5	0.1
Fibre diameter (µm)	0.5	15.3	20.8	28.6	3.0	0.5	13.3	20.5	28.5	2.6	0.5	0.0
Fibre lumina (µm)	0.8	2.4	6.2	12.1	2.0	0.8	2.6	5.2	11.0	1.4	0.8	0.2
Fibre length (µm)	0.7	641.8	1345.0	1878.3	220.3	0.6	767.5	1371.7	1861.1	217.5	0.7	0.0
Fibre wall thickness (µm)	0.6	4.1	7.3	10.3	1.3	0.6	4.4	7.6	10.3	1.2	0.6	0.0
Parenchyma strand length (number of cells)	0.8	2.0	6.6	13.0	2.2	0.8	2.0	5.5	9.0	1.6	0.8	0.2
Parenchyma strand length (µm)	**0.8**	195.7	562.7	1036.5	152.6	**0.8**	145.3	481.5	800.7	154.0	**0.9**	0.1
Rays frequency (Rays/mm')	0.7	5.0	10.9	17.0	2.5	0.7	7.0	13.5	21.0	3.3	0.8	0.2
Ray heigth (µm)	0.8	139.3	380.1	836.7	138.5	0.8	195.2	426.3	910.0	147.6	0.8	0.1
Ray width (µm)	0.7	12.8	23.4	38.4	4.6	0.7	8.0	19.7	29.0	4.4	0.8	0.2
Vessels percentage (%)	0.2	14.0	15.0	17.1	1.4	0.3	14.3	16.3	20.0	2.6	0.3	0.1
Fibres percentage (%)	0.4	15.9	21.0	25.4	4.3	0.1	28.1	31.0	33.0	2.4	0.5	0.3
Rays percentage (%)	0.2	31.5	35.5	38.0	3.1	0.1	32.0	35.1	36.7	2.1	0.2	0.0
Axial parenchyma percentage (%)	**0.2**	26.0	28.5	31.6	2.4	**0.3**	15.1	17.6	21.8	3.0	**0.5**	0.4
Wood density (g/cm3)	0.3	0.7	0.9	1.0	0.1	0.1	1.1	1.1	1.1	0.0	0.4	0.2
Vulnerability index	1.6					1.3						
Mesomorphy index	1143.8					1048.8						

Species	*E. cuspidifolium*											
Sites	Edge					Interior					Total PVI	PPI
Quantitative variables	PVI	MIN	M	MAX	SD	PVI	MIN	M	MAX	SD		
Vessel frequency (Vessels/mm^2)	**0.6**	41.0	66.7	107.0	20.0	**0.6**	65.0	98.3	157.0	25.9	**0.7**	0.3
Length vessel (µm)	0.7	317.6	658.3	913.5	129.5	0.7	296.2	694.7	1071.8	165.7	0.7	0.1
Vessel tangential diameter (µm)	0.6	27.2	52.3	75.3	11.6	0.5	32.0	50.6	67.2	7.2	0.6	0.0
Vessel radial diameter (µm)	0.6	38.4	61.7	94.4	13.3	0.5	35.2	56.2	76.8	8.9	0.6	0.1
Estimated vessel area (µm)	0.9	886.5	2614.7	6303.7	1208.2	0.7	1256.3	2441.0	4440.3	613.5	0.9	0.1
Vessel wall thickness (µm)	0.6	1.4	2.5	3.5	0.4	0.6	1.6	2.6	3.7	0.5	0.6	0.0
Intervessel pit heigth (µm)	**0.3**	3.3	4.1	4.8	0.4	**0.3**	3.7	4.5	5.5	0.4	**0.4**	0.1
Intervessel pit width (µm)	**0.3**	3.8	4.6	5.4	0.5	**0.3**	4.4	5.2	6.3	0.5	**0.4**	0.1
Vessel-ray pit heigth (µm)	0.6	3.9	6.9	10.5	2.0	0.7	3.2	5.9	10.4	1.9	0.7	0.1
Vessel-ray pit width (µm)	**0.6**	5.9	10.1	14.3	2.9	**0.6**	7.3	12.9	20.6	4.4	**0.7**	0.2
Vessel-parenchyma pit heigth (µm)	0.4	2.6	3.5	4.1	0.4	0.5	2.4	3.7	4.5	0.5	0.5	0.0
Vessel-parenchyma pit width (µm)	0.3	3.1	3.7	4.4	0.3	0.5	2.9	4.1	5.7	0.6	0.5	0.1
Fibre diameter (µm)	0.6	9.9	17.4	23.4	3.2	0.4	13.0	16.7	22.7	2.2	0.6	0.0
Fibre lumina (µm)	0.8	1.3	3.5	7.8	1.3	0.9	1.7	5.2	12.5	1.8	0.9	0.3
Fibre length (µm)	0.6	725.7	1199.0	1759.0	219.6	0.6	751.4	1300.4	1811.1	210.1	0.6	0.1
Fibre wall thickness (µm)	0.6	3.7	6.9	9.0	1.3	0.6	3.5	5.8	8.5	1.0	0.6	0.2
Parenchyma strand length (number of cells)	0.9	1.0	4.4	12.0	1.9	0.8	2.0	4.7	9.0	1.7	0.9	0.1
Parenchyma strand length (µm)	0.7	228.8	525.1	766.4	128.6	0.7	261.6	503.9	768.8	135.0	0.7	0.0
Rays frequency (Rays/mm')	0.5	6.0	10.2	13.0	1.6	0.6	5.0	8.8	13.0	1.9	0.6	0.1
Ray heigth (µm)	0.8	184.0	357.7	796.7	125.3	0.8	195.2	455.6	832.3	122.2	0.8	0.2
Ray width (µm)	0.8	8.0	20.3	32.0	4.9	0.7	11.3	22.3	35.3	5.3	0.8	0.1
Vessels percentage (%)	0.3	20.0	24.6	30.3	5.2	0.4	33.7	45.3	60.3	11.0	0.7	0.5
Fibres percentage (%)	**0.5**	13.3	17.3	25.0	6.7	**0.5**	8.9	13.4	18.3	4.2	**0.6**	0.2
Rays percentage (%)	0.3	27.0	30.9	36.1	4.7	0.4	20.5	27.4	33.9	6.6	0.4	0.1
Axial parenchyma percentage (%)	0.1	26.4	27.2	28.0	0.8	0.8	8.3	18.7	36.4	12.3	0.8	0.3
Wood density (g/cm3)	0.1	0.8	0.9	0.9	0.1	0.2	0.6	0.7	0.8	0.1	0.3	0.2
Vulnerability index	0.9					0.6						
Mesomorphy index	583.2					387.9						

are considered more vulnerable to embolism (Carlquist, 1977). Therefore, these species invest in greater vessel frequency when in stressful conditions, as also reported for other tree species (e.g., Drew and Pammenter, 2006; Pfautsch et al., 2016), since the negative effects of drought stress on xylem functionality are reduced with increased vessel frequency (Knipfer et al., 2015). On the other hand, AP species showed lower vessel frequency at edges and have vessel elements with lower vulnerability indexes compared to PP species. Therefore, these vessel elemewnts conduct less water, but in a more secure way (Hacke et al., 2006). In addition, AP species have a higher frequency of rays, which are cells involved in the maintenance of water flow (Morris et al., 2016b). This higher frequency of rays in AP species, combined with an increased percentage of apotracheal parenchyma in edge individuals, makes contact between parenchyma cells and vessel elements possible, since apotracheal parenchyma is arranged in networks that contacts vessel elements in some wood regions (Morris and Jansen, 2016).

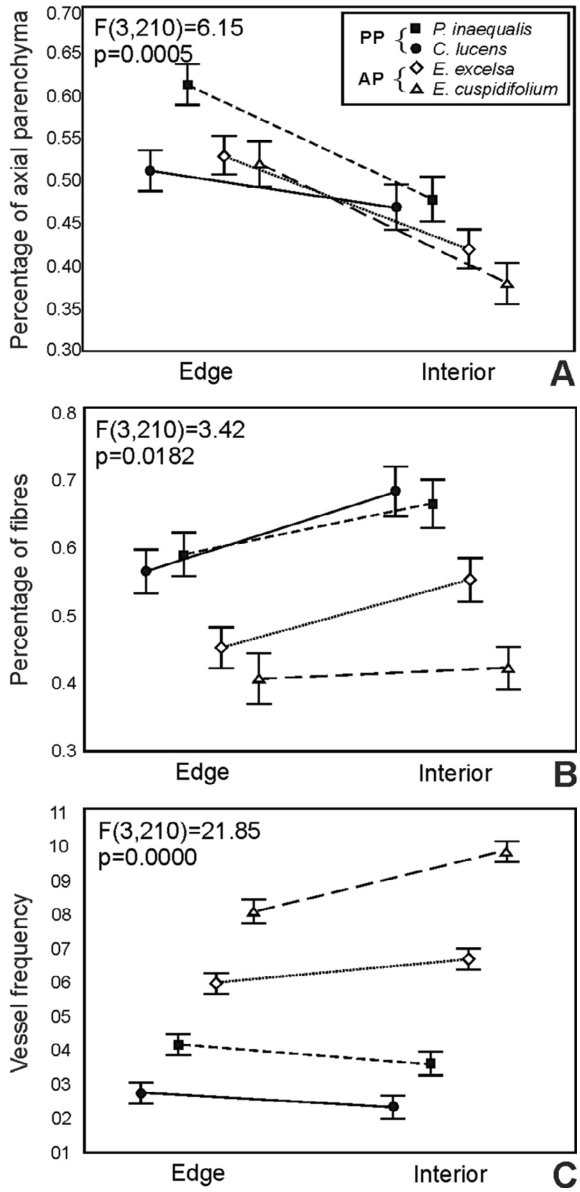

Fig. 5. Factorial ANOVA was performed to investigate the relationship between the selected species and the study areas and to understand general tendencies in the wood anatomy of these species. A – General tendencies in the percentage of axial parenchyma. B – General tendencies in fibre percentage. C – General tendencies in vessel frequency. Degrees of freedom and F and p values are provided for each graph. Vertical bars denote 95% confidence intervals.

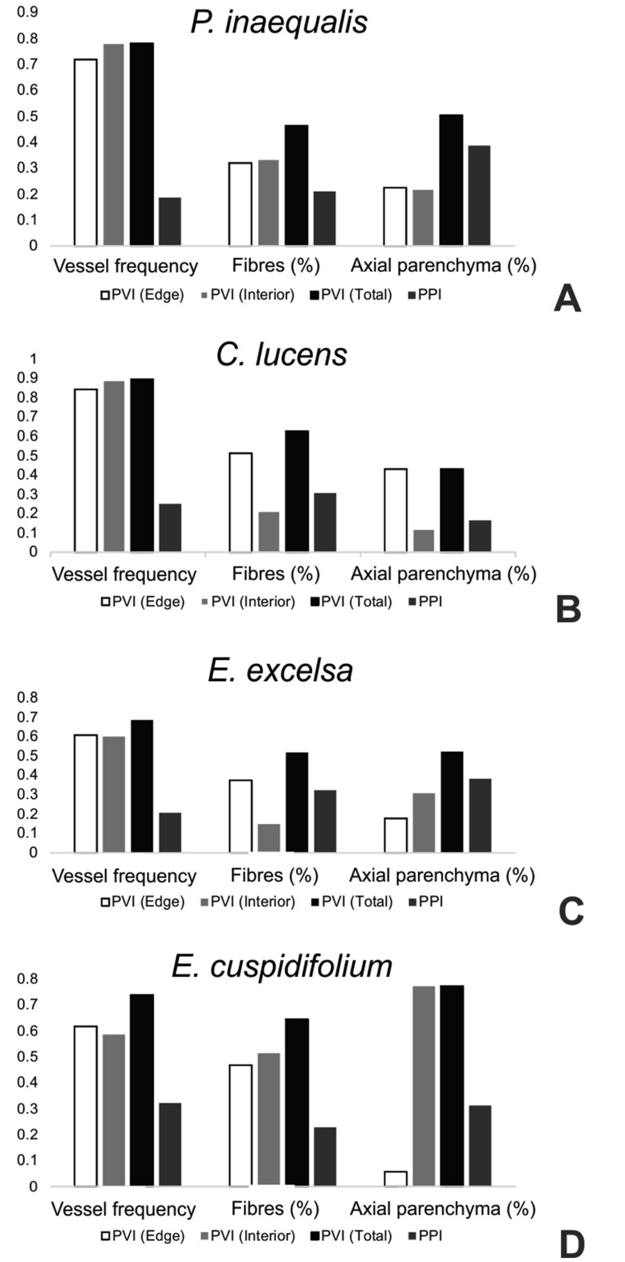

Fig. 6. Phenotypic variability index (PVI) for edge (white) and interior (light grey), total PVI (black) and phenotypic plasticity index (PPI) (dark grey). The indexzes are provided for vessel frequency, fibre percentage and axial parenchyma percentage in *P. inaequalis* (A), *C. lucens* (B), *E. excelsa* (C) and *E. cuspidifolium* (D).

Contact of one or a few parenchyma cells is sufficient for the re-establishment of water flow, since they can also act locally (Carlquist, 2015). The reduction of vessel frequency in individuals from forest edges shows that AP species under stressful conditions do not invest in more tracheary cells, but only in the parenchyma, which probably ensures the reversal of embolisms due to the role of parenchymatic cells (see Spicer, 2014).

Poorter et al. (2010) presented two orthogonal axes of variation in wood attributes: a primary axis related to the number and size of vessels, reflecting conductance in relation to hydraulic safety, and a secondary axis related to investment in the development of different tissues, which requires further investigation. PP species follow the first axis suggested by Poorter et al. (2010), while AP species invest in the formation of axial parenchyma and rays. These results suggest the existence of two functional groups based on the strategy for adjusting the xylem arrangement according to environmental changes, such as species in areas under edge effects. The anatomical adjustments to the xylem arrangement found for the two functional groups, indicate that xylem networks are not simply a set of empty dead cells, but a living and dynamic tissue able to respond to environmental variation caused by edge effects.

Tree species in different stressful environmental conditions invest in parenchymatic tissues (e.g., Vasconcellos et al., 2017; Secchi et al., 2016). Thus, the versatility of parenchyma cells needs more attention in a scenario of global climate change. Our results open an additional question about the future of tropical forests: can tropical tree species with more parenchymatic tissues or tropical tree species with higher phenotypic plasticity of this attribute (parenchyma) have better fitness in the face of global climate change?

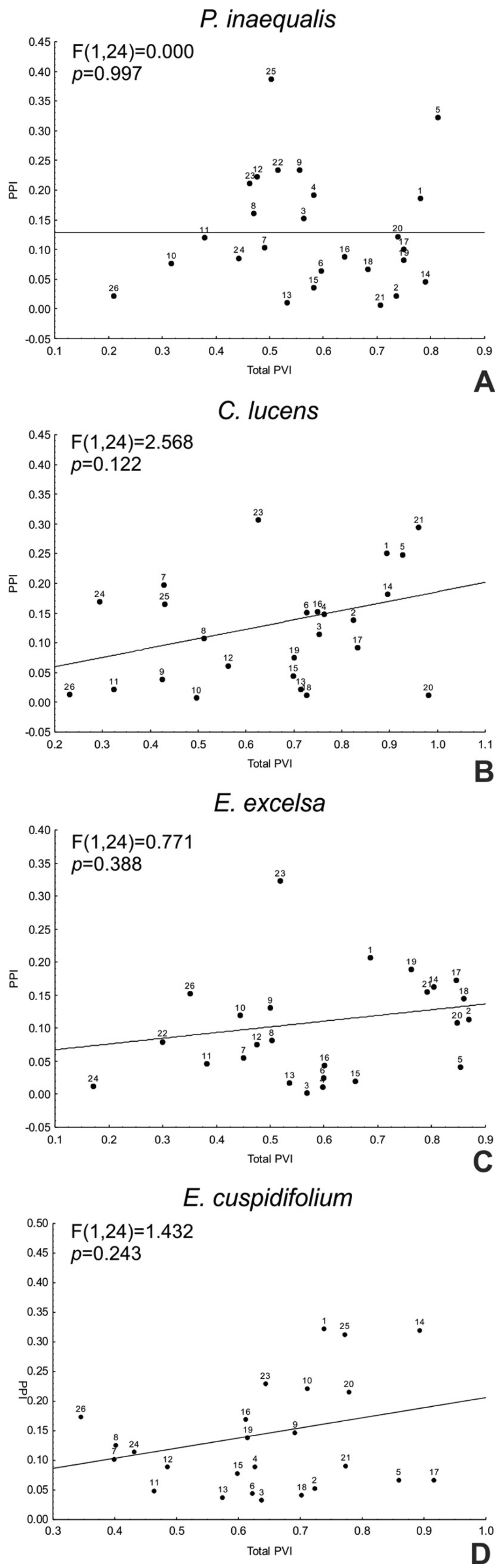

Fig. 7. Scatter plots, linear regression, and Spearman correlation statistics for the relationship between total PVI and PPI of wood anatomical traits of *P. inaequalis* (A), *C. lucens* (B), *E. excelsa* (C) and *E. cuspidifolium* (D). The variables (numbers) are listed in Table 2.

5. Conclusion

Our research has shed light on the influence that effects of forest edge have on wood functional anatomy. Tropical tree species shift to a greater abundance of axial parenchyma when subjected to effects of the forest edge. Our results corroborate that tree species in different stressful environmental conditions invest in parenchymatic tissues, probably because of the versatility of parenchyma cells. The distribution of axial parenchyma and its relationship to other different cell types of wood show two xylem arrangements that respond to edge effects with distinct trends in vessel frequency. In this way, hydraulic conduction in wood should not be understood as an entirely physical process occurring in vessel elements, but as a complex, integrated process operating among distinct cell types of wood. This complex cellular network composes unique xylem arrangements that need greater attention from functional, ecological, physiological, and evolutionary point of view.

Funding

This work was supported by Coordenação de Aperfeiçoamento de Pessoal de Nível Superior - Brasil (CAPES) - Finance Code 001; Conselho Nacional de Desenvolvimento Científico e Tecnológico (CNPq); and Fundação de Amparo à Pesquisa do Rio de Janeiro (FAPERJ); Rede de Pesquisas PPBio Mata Atlântica – Brasil (PPBio-Ma).

CRediT authorship contribution statement

Warlen Silva Costa: Methodology, Investigation, Formal analysis, Data curation, Writing - original draft. **Maura Da Cunha:** Conceptualization, Resources, Funding acquisition, Supervision, Writing - review & editing. **Pablo José F. Pena Rodrigues:** Resources, Writing - review & editing. **Mariana Andrade Iguatemy:** Visualization, Data curation, Writing - review & editing. **Fernando Valladares:** Methodology, Writing - review & editing. **Claudia Franca Barros:** Conceptualization, Resources, Funding acquisition, Validation, Writing - review & editing.

Declaration of Competing Interest

The authors declare that they have no known competing financial interests or personal relationships that could have appeared to influence the work reported in this paper.

Acknowledgments

We thank Erik Wild for linguistic advice. We thank Instituto de Pesquisas Jardim Botânico do Rio de Janeiro - Brasil for providing laboratory infrastructure. We thank Fernanda Negreiros for helping organize expeditions and fieldwork. We are also grateful to the technicians Elaine Zózimo and Rogério Figueiredo for their help with lab preparation, and Ivo P. Leme, Adilson Pintor and Jorge Caruso, for their help during fieldwork. We also thank Tahysa M. Macedo and Bruna Nunes de Luna for their helpful suggestions on the manuscript. This study is a part of the PhD thesis of the first author carried out at Programa de Pós-graduação em Biociências e Biotecnologia (UENF).

Appendix A. Supplementary data

Supplementary data to this article can be found online at https://doi.org/10.1016/j.foreco.2020.118305.

References

Alves, E.S., Angyalossy-Alfonso, V., 2000. Ecological trends in the wood anatomy of some brazilian species. 1. Growth rings and Vessels. IAWA J. 21, 3–30. https://doi.org/10.

1163/22941932-90000233.
Agpaua, D.M.G., Tng, D.Y.P., Cernusak, L.A., Cheesman, A.W., Santos, R.M., Edwards, W.J., Laurance, S.G.W., 2017. Plant functional groups within a tropical forest exhibit different wood functional anatomy. Funct. Ecol. 31, 582–591. https://doi.org/10.1111/1365-2435.12787.
Aubin, I., Munson, A.D., Cardou, F., 2016. Traits to stay, traits to move: a review of functional traits to assess sensitivity and adaptive capacity of temperate and boreal trees to climate change. Environ. Rev. 24, 1–23. https://doi.org/10.1139/er-2015-0072.
Baas, P., Schweingruber, F.H., 1987. Ecological trends in the wood anatomy of trees, shrubs and climbers from Europe. IAWA J. 8, 245–274. https://doi.org/10.1163/22941932-90001053.
Barros, C.F., Callado, C.H., Marcon, M.L., Costa, C.G., Cunha, M., Lima, H.R.P., 2001. Madeiras da Mata Atlântica: anatomia do lenho de espécies ocorrentes nos remanescentes florestais do estado do Rio de Janeiro – Brasil. Instituto de Pesquisas Jardim Botânico do Rio de Janeiro, Rio de Janeiro.
Bastias, C.C., Fortunel, C., Valladares, F., Baraloto, C., Benavides, R., Cornwell, W., Markesteijn, L., Oliveira, A.A., Sansevero, J.B.B., Vaz, M.C., Kraft, N.J.B., 2017. Intraspecific leaf trait variability along a boreal-to-tropical community diversity gradient. PLoS One. 27, 1–16. https://doi.org/10.1371/journal.pone.0172495.
Beeckman, H., 2016. Wood anatomy and trait-based ecology. IAWA J. 37, 127–151. https://doi.org/10.1163/22941932-20160127.
Bradshaw, A.D., 1965. Evolutionary significance of phenotypic plasticity in plants. Adv. Genet. 13, 115–155. https://doi.org/10.1016/S0065-2660(08)60048-6.
Brodersen, C.R., McElrone, A.J., 2013. Maintenance of xylem network transport capacity: a review of embolism repair in vascular plants. Front. Plant Sci. 108, 1–11. https://doi.org/10.3389/fpls.2013.00108.
Brodersen, C.R., Roddy, A.B., Wason, J.W., McElrone, A.J., 2019. Functional status of xylem through time annual. Annu. Rev. Plant Biol. 70, 21.1-21.27. https://doi.org/10.1146/annurev-arplant-050718-100455.
Bukatsch, F., 1972. Bemerkungen zur doppelfärbung astrablau-safranin. Mikrokosmos 61, 33–36.
Burger, L.M., Richter, H.G., 1991. Anatomia da Madeira. Nobel, São Paulo.
Carlquist, S., 1977. Ecological factors in wood evolution: a floristic approach. Am. J. Bot. 64, 887–896. https://doi.org/10.2307/2442382.
Carlquist, S., 1988. Comparative wood anatomy: systematic, ecological and evolutionary aspects of dicotyledon wood. Springer-Verlag, Berlin.
Carlquist, S., 2015. Living cells in wood. 1. Absence, scarcity and histology of axial parenchyma as keys to function. Bot. J. Linn. Soc. 177, 291–321. https://doi.org/10.1111/boj.12247.
Carlquist, S., 2018. Living Cells in Wood 3. Overview; Functional Anatomy of the Parenchyma Network. Bot. Rev. 84, 242–294. https://doi.org/10.1007/s12229-018-9198-5.
Drew, D.M., Pammenter, N.W., 2006. Vessel frequency, size and arrangement in two eucalypt clones growing at sites differing in water availability. Nz. J. Forestry Sci. 51, 23–28.
Fonti, P., Arx, G., García-González, I., Eilmann, B., Sass-Klaassen, U., Gärtner, H., Eckstein, D., 2010. Studying global change through investigation of the plastic responses of xylem anatomy in tree rings. New Phytol. 185, 42–53. https://doi.org/10.1111/j.1469-8137.2009.03030.x.
Galindo-Leal, C., Câmara, E., 2005. Status do hotspot Mata Atlântica: uma síntese. In: Galindo-Leal, C., Rodrigues, E. (Eds.), Mata Atlântica: Biodiversidade, Ameaças e Perspectivas. Fundação SOS Mata Atlântica Conservação Internacional, São Paulo, pp. 03–11.
Gianoli, E., Valladares, F., 2012. Studying phenotypic plasticity: the advantages of a broad approach. Biol. J. Linn. Soc. 105, 1–7. https://doi.org/10.1111/j.1095-8312.2011.01793.x.
Gratani, L., 2014. Plant phenotypic plasticity in response to environmental factors. Advances in Botany. 2014, 1–17. https://doi.org/10.1155/2014/208747.
Grissino-Mayer, H.D., 2003. A manual and tutorial for theproper use of an increment borer. Tree-Ring Res. 59, 63–79.
Hacke, U.G., Sperry, J.S., Wheeler, J.K., Castro, L., 2006. Scaling of angiosperm xylem structure with safety and efficiency. Tree Physiol. 26, 689–701. https://doi.org/10.1093/treephys/26.6.689.
Haddad, N.M., Brudvig, L.A., Clobert, J., Davies, K.F., Gonzalez, A., Holt, R.D., Lovejoy, T.E., Sexton, J.O., Austin, M.P., Collins, C.D., Cook, W.M., Damschen, E.I., Ewers, R.M., Foster, B.L., Jenkins, C.N., King, A.J., Laurance, W.F., Levey, D.J., Margules, C.R., Melbourne, B.A., Nicholls, A.O., Orrock, J.L., Song, D., Townshend, J.R., 2015. Habitat fragmentation and its lasting impact on earth's ecosystems. Sci. Adv. 20, 1–9. https://doi.org/10.1126/sciadv.1500052.
Committee, I.A.W.A., 1989. IAWA list of microscopic feature for hardwood identification. IAWA J. 10, 219–332. https://doi.org/10.1163/22941932-90000496.
Jane, F.W., 1956. The structure of wood. Adam e Black, Londres.
Johansen, D.D., 1940. Plant microtechniques. McGraw-Hill, New York.
Jupa, R., Plavcová, L., Gloser, V., Jansen, S., 2016. Linking xylem water storage with anatomical parameters in five temperate tree species. Tree Physiol. 00, 1–14. https://doi.org/10.1093/treephys/tpw020.
Knipfer, T., Brodersen, C.R., Zedan, A., Kluepfel, D.A., McElrone, A.J., 2015. Patterns of drought-induced embolism formation and spread in living walnut saplings visualized using X-ray microtomography. Tree Physiol. 00, 1–12. https://doi.org/10.1093/treephys/tpv040.
Lachenbruch, B., McCulloh, K.A., 2014. Traits, properties, and performance: how woody plants combine hydraulic and mechanical functions in a cell, tissue, or whole plant. New Phytol. 204, 747–764. https://doi.org/10.1111/nph.13035.
Laurance, W.F., Delamônica, P., Laurance, S.G., Vasconcelos, H.L., Lovejoy, T.E., 2000. Rainforest fragmentation kills big trees. Nature 404, 836. https://doi.org/10.1038/35009032.
MacArthur, R., Levins, R., 1967. The limiting similarity, convergence, and divergence of coexisting species. Am. Nat. 101, 377–385.
Metcalfe, C.R., Chalk, L., 1950. Anatomy of Dicotyledons. Clarendon Press, Oxford.
Metzger, J.P., Martensen, A.C., Dixo, M., Bernacci, L.C., Ribeiro, M.C., Teixeira, M.G., Pardini, R., 2009. Time-lag in biological responses to landscape changes in a highly dynamic Atlantic forest region. Biol. Conserv. 142, 1166–1177. https://doi.org/10.1016/j.biocon.2009.01.033.
Mittermeier, R.A., Robles, P.G., Hoffmann, M., Pilgrim, J., Brooks, T., Mittermeier, C.M., Lamoreux, J., Da Fonseca, G.A.B., 2004. Hotspots revisited: Earth's biologically richest and most endangered terrestrial ecoregions. Conservation International and Agrupacio'n Sierra Madre, Monterrey, Mexico.
Morris, H., Jansen, S., 2016. Secondary xylem parenchyma from classical terminology to functional traits. IAWA J. 37, 1–15. https://doi.org/10.1163/22941932-20160117.
Morris, H., Brodersen, C., Schwarze, F.M.W.R., Jansen, S., 2016a. The parenchyma of secondary xylem and its critical role in tree defense against fungal decay in relation to the CODIT model. Front. Plant Sci. 7, 1–18. https://doi.org/10.3389/fpls.2016.01665.
Morris, H., Plavcova, L., Cvecko, P., Fichtler, E., Gillingham, M.A.F., Martínez-Cabrera, H.I., McGlinn, D.J., Wheeler, E., Zheng, J., Zieminska, K., Jansen, S., 2016b. A global analysis of parenchyma tissue fractions in secondary xylem of seed plants. New Phytol. 209, 1553–1565. https://doi.org/10.1111/nph.13737.
Morris, H., Gillingham, M.A.F., Plavcová, L., Gleason, S.M., Olson, M.E., Coomes, D.A., Fichtler, E., Klepsch, M.M., Martinez-Cabrera, H.I., Glinn, D.J., Wheeler, E.A., Zheng, J., Zieminska, K., Jansen, S., 2018. Vessel diameter is related to amount and spatial arrangementof axial parenchyma in woody angiosperms. Plant Cell Environ. 41, 245–260. https://doi.org/10.1111/pce.13091.
Morris, H., Hietala, A.M., Jansen, S., Ribera, J., Rosner, S., Salmeia, K.A., Schwarze, F.W.M.R., 2019. Using the CODIT model to explain secondary metabolites of xylem in defence systems of temperate trees against decay fungi. Ann. Bot. 138, 1–20. https://doi.org/10.1093/aob/mcz138.
Olson, M.E., Rosell, J.A., 2013. Vessel diameter–stem diameter scaling across woody angiosperms and the ecological causes of xylem vessel diameter variation. New Phytol. 197, 1204–1213. https://doi.org/10.1111/nph.12097.
Olson, M.E., Anfodillo, T., Rosell, J.A., Petit, G., Crivellaro, A., Isnard, S., León-Gómez, C., Alvarado-Cárdenas, L.O., Castorena, M., 2014. Universal hydraulics of the flowering plants: vessel diameter scales with stem length across angiosperm lineages, habits and climates. Ecol. Lett. 17, 988–997. https://doi.org/10.1111/ele.12302.
Pfautsch, S., Harbusch, M., Wesolowski, A., Smith, R., Macfarlane, C., Tjoelker, M.G., Reich, P.B., Adams, M.A., 2016. Climate determines vascular traits in the ecologically diverse genus *Eucalyptus*. Ecol. Lett. 19, 240–248. https://doi.org/10.1111/ele.12559.
Plavcová, L., Hoch, G., Morris, H., Ghiasi, S., Jansen, S., 2016. The amount of parenchyma and living fibers affects storage of nonstructural carbohydrates in young stems and roots of temperate trees. Am. J. Bot. 103, 1–10. https://doi.org/10.3732/ajb.1500489.
Pohlman, C.L., Turton, S.M., Goosem, M., 2007. Edge effects of linear canopy openings on tropical rain forest understory microclimate. Biotropica 39, 62–71. https://doi.org/10.1111/j.1744-7429.2006.00238.x.
Poorter, L., McDonald, I., Alarco, A., Fichtler, E., Licona, J.C., Peña-Claros, M., Sterck, F., Villegas, Z., Sass-Klaassen, U., 2010. The importance of wood traits and hydraulic conductance for the performance and life history strategies of 42 rainforest tree species. New Phytol. 185, 481–492. https://doi.org/10.1111/j.1469-8137.2009.03092.x.
Prieto, P.V., Sansevero, J.B.B., Garbin, M.L., Braga, J.M.A., Rodrigues, P.J.F.P., 2013. Edge Effects of Linear Canopy Openings on Understory Communities in a Lowland Atlantic Tropical Forest. Appl. Veg. Sci. 17, 121–128. https://doi.org/10.1111/avsc.12043.
R CORE TEAM, 2018. R: A language and environment for statistical computing. R Foundation for Statistical Computing, Vienna, Austria. http://www.R-project.org/ (accessed 15 March 2018).
Rezende, C.L., Scarano, F.R., Assad, E.D., Joly, C.A., Metzger, J.P., Strassburg, B.B.N., Tabarelli, M., Fonseca, G.A.B., Mittermeier, C.G., 2018. From hotspot to hopespot: An opportunity for the Brazilian Atlantic Forest. Perspect. Ecol. Conser. 16, 208–214. https://doi.org/10.1016/j.pecon.2018.10.002.
Ribeiro, M.C., Metzeger, J.P., Martensen, A.C., Ponzni, M.M.H., 2009. The Brazilian Atlantic Forest: how much is left, and how is the remaining forest distributed? implications for conservation. Biol. Conserv. 142, 1141–1153. https://doi.org/10.1016/j.biocon.2009.02.021.
Rodrigues, P.J.F.P., Iguatemy, M.A., Prieto, P.V., Reis, T.S., Sansevero, J.B.B., Simões-Jesus, M.F., 2008. As pesquisas no longo prazo em parcelas permanentes do Jardim Botânico do Rio de Janeiro. In: Sanquetta, C.R. (Ed.), Experiências de monitoramento no Bioma Mata Atlântica com uso de parcelas permanentes. Rede Map Press, Curitiba, pp. 47–80.
Rodrigues, P.J.F.P., Melo, L.R., Abreu, R.C.R., Iguatemy, M.A., 2016. Edge Effects of Oil Pipeline Canopy Openings on Tree Community Structure and Dynamics in a Montane Atlantic Forest. Journal of Geoscience and Environment Protection 4, 132–140. https://doi.org/10.4236/gep.2016.47014.
Sass, J.E., 1958. Elements of botanical microtechnique. Mc. Graw-Hill Book Company Inc., New York-London.
Scarano, F.R., Ceotto, P., 2015. Brazilian Atlantic forest: impact, vulnerability, and adaptation to climate change. Biodivers. Conserv. 24, 2319–2331. https://doi.org/10.1007/s10531-015-0972-y.
Secchi, F., Pagliarani, C., Zwieniecki, M.A., 2016. The functional role of xylem parenchyma cells and aquaporins during recovery from severe water stress. Plant Cell Environ. 40, 858–871. https://doi.org/10.1111/pce.12831.

Silva, W.G.S., Metzger, J.P., Simões, S., Simonetti, C., 2007. Relief influence on the spatial distribution of the Atlantic Forest cover at the Ibiúna Plateau. SP. Braz. J. Biol. 67, 403–411. https://doi.org/10.1590/S1519-69842007000300004.
Simões de Jesus, M.F., 2009. Análise dos efeitos de borda sobre a composição, dinâmica e estrutura da comunidade arbórea na Mata Atlântica da Reserva Biológica do Tinguá–RJ. Master's Thesis, Escola Nacional de Botânica Tropical, Instituto de Pesquisas Jardim Botânico do Rio de. Janeiro, Brasil.
Sonsin, J.O., Gasson, P., Barros, C.F., Marcati, C.R., 2012. A comparison of the wood anatomy of 11 species from two cerrado habitats (cerrado s.s. and adjacent gallery forest). Bot. J. Linn. Soc. 170, 257–276. https://doi.org/10.1111/j.1095-8339.2012.01282.x.
Sperry, J.S., Hacke, U.G., Pittermann, J., 2006. Size and function in conifer tracheids and angiosperm vessel. Am. J. Bot. 93, 1490–1500. https://doi.org/10.3732/ajb.93.10.1490.
Spicer, R., 2014. Symplasmic networks in secondary vascular tissues: parenchyma distribution and activity supporting long-distance transport. J. Exp. Bot. 65, 1829–1848. https://doi.org/10.1093/jxb/ert459.
Statsoft, 1993. Statistica: Statsoft for windows: General conventions and statistics I. User's Handbook. Microsoft Corporation, Tulsa.
Stranburger, E., 1924. Handbook of practical botany. MacMillan Company, New York.
Sun, Q., Rost, T.L., Matthews, M.A., 2008. Wound-induced vascular occlusions in *Vitis vinifera* (Vitaceae): tyloses in summer and gels in winter. Am. J. Bot. 95, 1498–1505. https://doi.org/10.3732/ajb.0800061.
Valladares, F., Sanchez-Gomez, D., Zavalat, M.A., 2006. Quantitative estimation of phenotypic plasticity: bridging the gap between the evolutionary concept and its ecological applications. J. Ecol. 94, 1103–1116. https://doi.org/10.1111/j.1365-2745.2006.01176.x.
Vasconcellos, T.J., Cunha, M., Callado, C.H., 2017. A comparative study of cambium histology of *Ceiba speciosa* (A. St.-Hil.) Ravenna (Malvaceae) under urban pollution. Environ. Sci. Pollut. R. 24, 12049–12062. https://doi.org/10.1007/s11356-015-6012-3.
Violle, C., Navas, M.L., Vile, D., Kazakou, E., Fortunel, C., Hummel, I., Garnier, E., 2007. Let the concept of trait be functional!. Oikos 116, 882–892. https://doi.org/10.1111/j.2007.0030-1299.15559.x.
Weinzettel, J., Vackár, D., Medková, H., 2018. Human footprint in biodiversity hotspots. Front. Ecol. Environ. 16, 447–452. https://doi.org/10.1002/fee.1825.
Wheeler, E.A., Baas, P., 1991. A survey of the fossil record for dicotyledonous wood and its significance for evolutionary and ecological wood anatomy. IAWA J. 12, 275–332. https://doi.org/10.1163/22941932-90001256.
Zanne, A.E., Westoby, M., Falster, D.S., Ackerly, D.D., Loarie, S.R., Arnold, S.E.J., Coomes, D.A., 2010. Angiosperm wood structure: global patterns in vessel anatomy and their relation to wood density and potential conductivity. Am. J. Bot. 97, 207–215. https://doi.org/10.3732/ajb.0900178.
Zar, J.H., 2010. Biostatistical analysis. Prentice Hall, Upper Saddle River.